

TORNADO-INDUCED WIND LOADS ON A COMMUNITY OF LOW-RISE BUILDINGS

Ruijia Yang

Department of Atmospheric and Oceanic Sciences
McGill University
805, rue Sherbrooke Ouest, Montréal, Québec
H3A 0B9, Canada
rui.yang@mail.mcgill.ca

Djordje Romanic

Department of Atmospheric and Oceanic Sciences
McGill University
805, rue Sherbrooke Ouest, Montréal, Québec
H3A 0B9, Canada
djordje.romanica@mcgill.ca

Horia Hangan

Department of Mechanical and Manufacturing Engineering
Ontario Tech University
2000 Simcoe Street North, Oshawa, Ontario
L1G 0C5, Canada
horia.hangan@ontariotechu.ca

ABSTRACT

An innovative wind chamber study on wind loads induced by tornado-like vortices (TLVs) on a realistic, geometrically complex built community is performed at the WindEEE Dome tornado simulator at Western University, Canada. The pressure distribution induced by the TLVs on the model buildings are quantified and compared to ASCE 7-22 building provisions. For each geometric configuration of the community, stationary EF1-, EF2- and EF3-rated TLVs are simulated. Flow aerodynamics are assessed by assessing time-averaged and instantaneous pressure coefficients. The spatial location of pressure minimums conform to pressure distribution observed from flow separation, with the roof experiencing the highest pressure deficits. Building interaction and sheltering effects are observed by varying the community geometry. The instantaneous pressures are subject to extreme value analyses, which identified return period pressure coefficients that can be compared with ASCE 7-22.

INTRODUCTION

Tornadoes are violently rotating columns of air capable of inflicting substantial life and property damages. In some years, total losses attributed to tornadoes in the United States (US) surpass that of hurricanes and other wind perils (Romanic *et al.*, 2016). In Canada, tornadoes are responsible for the highest average loss per catastrophe in both Ontario and Quebec between 2008 and 2021 (Hadavi *et al.*, 2022). Therefore, there is a great need to better understand tornadic effects on buildings to reduce their damage potential. Quantifying tornadic effects on buildings and other structures is still relatively lacking despite signs of progress, especially regarding flow aerodynamics (pressure distribution) and wind loading (aerodynamic forces exerted) (Roueche *et al.*, 2020). In particular, tornadic wind loading and actions on real buildings and communities show a significant lack of research.

Three main approaches in tornado resilience research

exist: (1) full-scale assessment from post-tornado damage surveys, (2) numerical modelling of tornadic vortices and their interaction with structures, and (3) physical simulations of tornado-like vortices (TLVs) in wind chambers (Romanic *et al.*, 2023b). Post-disaster damage surveys cannot yield the pressure distribution around the building prior to and at the instant of damage occurrence. Inconsistencies in estimating the wind speed can also arise (Lombardo *et al.*, 2015). In addition, the internal flow structure of the tornado vortex is difficult to assess without Doppler radar observations. Even in their presence, constraints of spatial coverage and possible debris contamination limit their usefulness (Nolan, 2013). Numerical simulations of TLVs currently lack proper estimates of velocity peaks and turbulence representation, both crucial in the wind loading and structural analyses (e.g. in Lewellen and Lewellen, 2007). While not perfect, physical wind chamber simulations of TLVs overcome most of those shortcomings.

Previous wind tunnel studies of TLVs were primarily focused on isolated or idealized cubic buildings. However, multiple buildings can produce sheltering and other effects, which are usually dependent on the size, orientation and fine-scale properties of the buildings (i.e., roof shape, edges, etc.). For example, Sabareesh *et al.* (2018) found that adjacent buildings induce internal and external pressure enhancement or reduction. Very few wind tunnel studies have been conducted for a community of complex, non-idealized building structures (e.g. Narancio *et al.*, 2023a). Finally, building provisions in the US have been insufficient in addressing tornadic wind loads. Only recently did the American Society of Civil Engineers (ASCE) start to address tornado-resistant designs (ASCE, 2022). The Canadian building code does not account for tornadic loads.

The current study presents the first physical simulation of surface pressures and aerodynamic forces exerted by EF1 to EF3-rated TLVs on realistic buildings, and in a community that is planned to be built in the state of Kansas (KS), US: the Kansas Project (KP). The KP site is 680 acres of pasture, meadows and buttes in south-central Kansas, US. The tornado

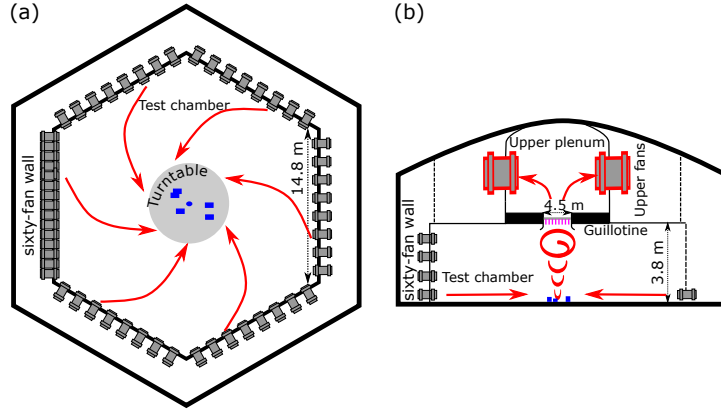


Figure 1. Schematics of the WindEEE Dome tornado mode, with the KP community in blue (not to scale).

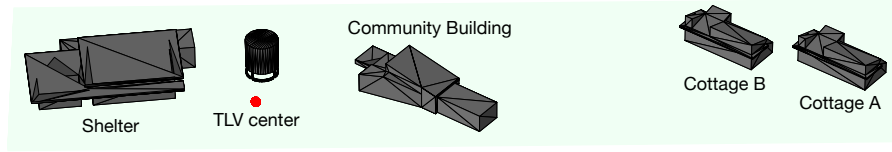


Figure 2. Overview of KP site for configuration 1. Cottage A's position can be adjusted for different configurations.

season on the site peaks in May, with a climatology of 2.6 tornadoes per year, 93% of which are estimated to be below EF2, and the deadliest at EF3 (Romanic *et al.*, 2018). KP's objectives are twofold: resilience and sustainability. To this end, the WindEEE Dome tornado simulator at Western Ontario (Hangan *et al.*, 2017) is employed to investigate tornado resilience of seven community layouts at the KP.

DATA AND METHODS

WindEEE Dome

The WindEEE Dome is a new-generation wind chamber designed to simulate TLVs, downburst-like and atmospheric boundary layer winds (Fig. 1a). TLVs are created using six large fans situated in the upper plenum and the directional louvers located along the periphery of the test chamber (Fig. 1b). The upper fans create the updraft using suction, while the louver vanes control the angle to provide a swirl in the flow (Refan and Hangan, 2018). Upper fan strengths and louver directions control various dynamic characteristics of a TLV.

The main parameters governing the dynamics of TLVs are swirl ratio S , aspect ratio a and radial Reynolds number Re_r :

$$S = \frac{\Gamma_{\max} r_0}{2Qh}; a = \frac{h}{r_0}; Re_r = \frac{Q}{2\pi v} \quad (1)$$

where $h = 0.8$ m is the inflow depth, $r_0 = 2.25$ m is the updraft radius, Γ_{\max} is the maximum circulation in the flow, and Q is the volumetric flow rate per unit length. The WindEEE Dome is capable of a wide range of geometric and velocity scales; a geometric scale of 1:100 is used in these experiments.

Experiments and pressure measurements

The KP community consists of four buildings: two cottages (Cottage A and Cottage B), a community centre (Community Building), and a tornado Shelter. Figure 2 shows the

layout of this community in one of the configurations. In all cases, the TLV was centered above the middle of the community. Various configurations adjust the location of Cottage A varied to consider the effects of building orientations from tornado center; the height of the Shelter; and the addition or removal of additional architectural elements such as pavilion and cantilevered deck for both Community Building and Shelter. Table 1 summarizes the tested configurations. Given the

Table 1. Summary of configurations tested. Fig. 2 shows configuration 1 and relative positions of individual buildings.

Config.	Position of Cottage A	Full scale Shelter height	Pavilion and obs. tower
1	1	3.8 m	Present
2	1	2.8 m	Present
3	1	1.8 m	Present
4	1	3.8 m	Absent
5	2	3.8 m	Present
6	3	3.8 m	Present

climatology at the KP site (as in Romanic *et al.*, 2018), EF1-, EF2- and EF3-rated tornadoes are modelled at the WindEEE Dome, each with different characteristic values of V_{tm} (maximum tangential velocity at core radius r_c , from Refan and Hangan, 2018), r_c and S , further detailed in Table 2. These physical parameters can yield the velocity scale, λ_v . From this, and the geometric scale λ_L , as previously discussed, the time scale λ_T can be obtained as $\lambda_T = \frac{\lambda_L}{\lambda_v}$. Therefore, for each configuration, 3 TLVs are modelled. In total, 430 pressure taps were installed on the walls and roofs of the buildings to collect pressure readings.

The pressure readings p_i , at tap i , are converted to pressure coefficients $C_{p,i}$ using a reference pressure p_{ref} represen-

Table 2. Main physical characteristics of TLVs used.

	V_{tm} (ms ⁻¹)	r_c (m)	S	λ_V	λ_T
EF1	12.8	0.42	0.59	1:3.4	1:29.4
EF2	13.8	0.60	0.69	1:4.0	1:25.0
EF3	16.2	0.69	1.03	1:4.1	1:24.4

tative of the ambient pressure during the experiment:

$$C_{p,i} = \frac{P_i - P_{ref}}{\frac{1}{2}\rho V_{tm}^2} \quad (2)$$

Using the time scale λ_T from table 2, 3-second moving averages of $C_{p,i}$ time series can be extracted. The moving average time series is then divided into smaller segments, an approach followed in Narancio *et al.* (2023b), albeit for velocity measurements. The length of the segment is chosen to represent a reasonable duration of a medium-lived tornado (Blair and Leighton, 2014), about 5 minutes in full scale. The effect of this length influences the analysis, but its effects were not investigated here. For each segment, the minimum 3-s average C_p value was determined. This subset of minimum C_p values is fit to a Gumbel distribution using the Best Linear Unbiased Estimator (BLUE) method (Lieblein, 1976):

$$F(x) = \exp\left(-\exp\left(-\frac{x-u}{a}\right)\right) \quad (3)$$

where $F(x)$ is the cumulative distribution function, x is the value of a random variable, and u and a are the location and scale parameters. The default ISO probabilities of non-exceedance are used for the fitting (ISO 4354:2009, 2000). The BLUE method allows to retrieve the “design value” from the Gumbel distribution expected value (Wang and Cao, 2021). Following similar analyses (Godlewski *et al.*, 2021; Hong *et al.*, 2013), the return period x_T is estimated from

$$x_T = u + a(-\ln(-\ln(1 - 1/T))) \quad (4)$$

The design pressures from ASCE 7-22 broadly fall into two categories: main wind force resisting system (MWFRS) and components & cladding (C&C) (ASCE, 2022). For each category, the building risk category is determined: given the vocation of KP structures, they are determined to be Category I. The external pressure coefficients can then be retrieved according to the building shape and size: Chapter 27 gives design C_p values for MWFRS, and Chapter 30 for C&C.

RESULTS

The time-averaged pressure coefficients, interpolated by radial basis functions, between and around the pressure taps, are shown in Figure 3 for Community Building in configuration 1, for EF3-rated TLV. Generally, maximum pressure deficits are observed near the edge of buildings, agreeing with previous wind tunnel and full-scale measurements (e.g. in Lin *et al.*, 1995 and Stathopoulos *et al.*, 1990). This suction can be attributed to flow separation (Ginger and Letchford, 1993).

In addition, the lowest pressure observed in figure 3 occurs on the roof, consistent with effects induced by TLVs. The location of this suction maximum is consistent between various configurations and TLV strengths, as shown in Figure 4. Generally, the lowest pressure observed occur on the roof, which can again be explained by flow separation around the sharp corners of the roof. In addition, it is of note that the magnitude of the pressure deficit decreases as the swirl ratio of TLV increases. Refan and Hangan (2018) performed the wind chamber test without buildings, and attributed this observed decrease in suction to the usage of tangential maximum velocity V_{tm} in obtaining pressure coefficients, because V_{tm} increases with the swirl ratio. They noted that the opposite holds true by considering the axial velocity. On the other hand, Haan *et al.* (2010) attributes this effect to the vortex breakdown occurring in stronger TLVs, asserting that the suction decreases with higher swirl ratio. A similar trend is observed for other configurations (not shown). Various aerodynamic effects associated with complex building geometries and wake effect caused by TLVs of different sizes and intensities could explain this difference between the contradicting results. However, this hypothesis requires further research.

Figure 5 shows the effect of altering building geometries. In the case where additional structures were removed from the shelter (figure 5a), some significant differences were noticed at the back of the building. This result may be due to the shelter building being more exposed after the pavilion was removed. When the shelter height was adjusted (figure 5b), there is no statistically-significant C_p differences observed. Finally, when Cottage A was moved further away from the TLV center (from position 1 to 3), the suction decreases as expected.

The probability density distributions are plotted for Community Building in configuration 1, for all 3 TLV strengths, as shown in figure 6. Panel (a) shows a pressure tap located in the middle of the back side, on a protruded portion, and panel (b) shows a tap located on the edge of this protrusion. The tap on the edge of this protrusion has noticeably less Gaussian distributions. For EF1- and EF2-rated TLVs, the distribution is bimodal. This could be attributed to flow separation associated with the complex building geometry. In addition, for both taps, the profile is broader and less Gaussian for weaker TLVs, consistent with Romanic *et al.* (2023a). This can be attributed to the fact that lower swirl ratio (weaker TLV) causes more wandering (Refan and Hangan, 2018). Both taps also show that with increasing swirl ratio, the suction decreases, consistent with results shown in figure 4. This similar trend of decreasing suction is also observed in other taps, buildings or configurations (not shown).

Figure 7 shows the return period obtained from BLUE method, after the Gumbel fit. The trend of the C_p return period is as expected: As Cottage A is farthest from TLV center, for a given return period, the C_p is less negative, consistent with the pressure profile expected from TLVs. Indeed, it has been shown that the BLUE method provides a reliable estimate of peak C_p values and return period analyses on several other occasions (e.g. Hong *et al.*, 2013; Godlewski *et al.*, 2021). Many previous analyses using the BLUE method mainly address wind measurement (e.g. in Hong *et al.*, 2013). In addition, for both Cottage A and Community Center, the roof experiences the strongest pressure deficit, agreeing with previous analyses. The magnitude of pressure deficit are generally strong compared to provisions such as ASCE 7-22. For comparison, components and cladding (C&C) external pressure coefficients for a flat roof is specified to be -3.2 at the corners of the roof ASCE (2022). This value fluctuates de-

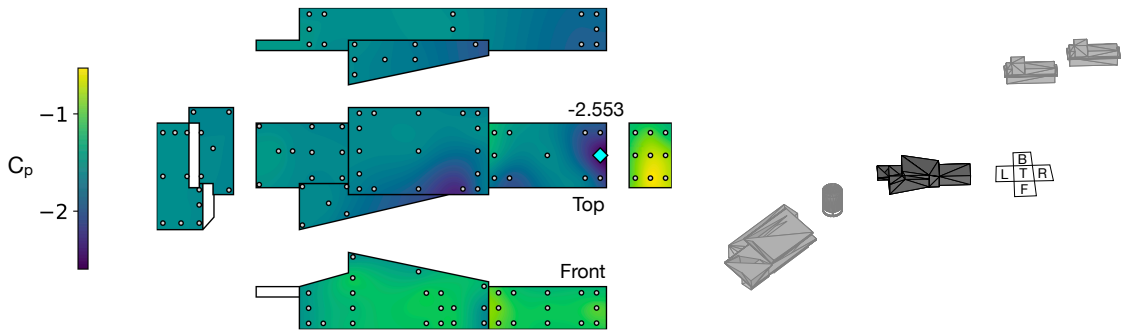


Figure 3. Exploded view of time-averaged pressure coefficient C_p for Community Building, configuration #1, EF3-rated TLV. The location of the building relative to the community is highlighted on the right, with faces corresponding to those in the exploded view.

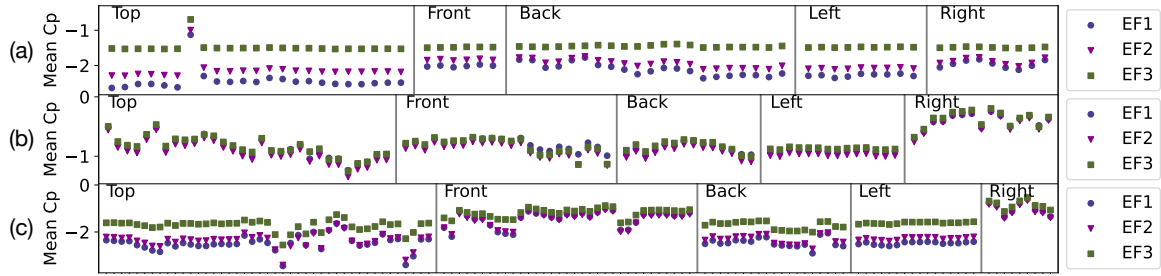


Figure 4. Time averaged pressure coefficient C_p in configuration 1 for all pressure taps, organized by the face where they are located, for EF1-, EF2- and EF3-rated TLVs, for (a) Shelter, (b) Cottage A and (c) Community Building.

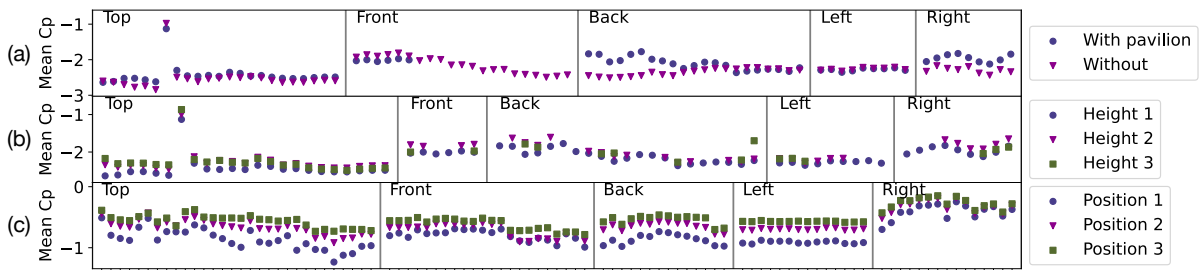


Figure 5. Time averaged pressure coefficient C_p for EF1-rated TLVs for all pressure taps, organized by their location on the building. (a) compares when additional structures are removed from Shelter; (b) compares various heights of the Shelter; and (c) compares the position of Cottage A.

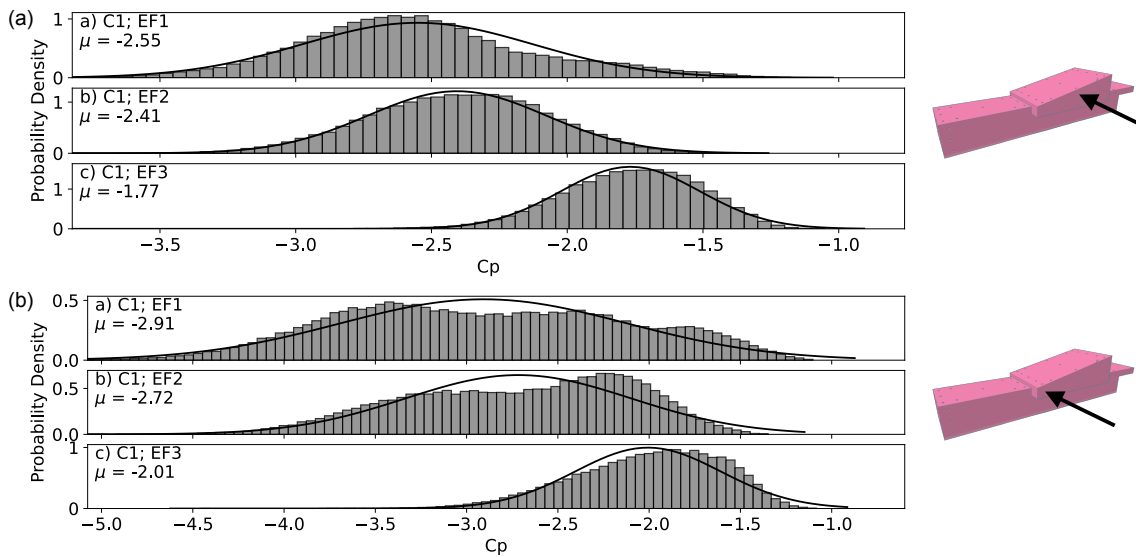


Figure 6. Probability density and Gaussian fit for taps (a) #931 and (b) #915, both located on the back side of Community Building, in configuration #1.

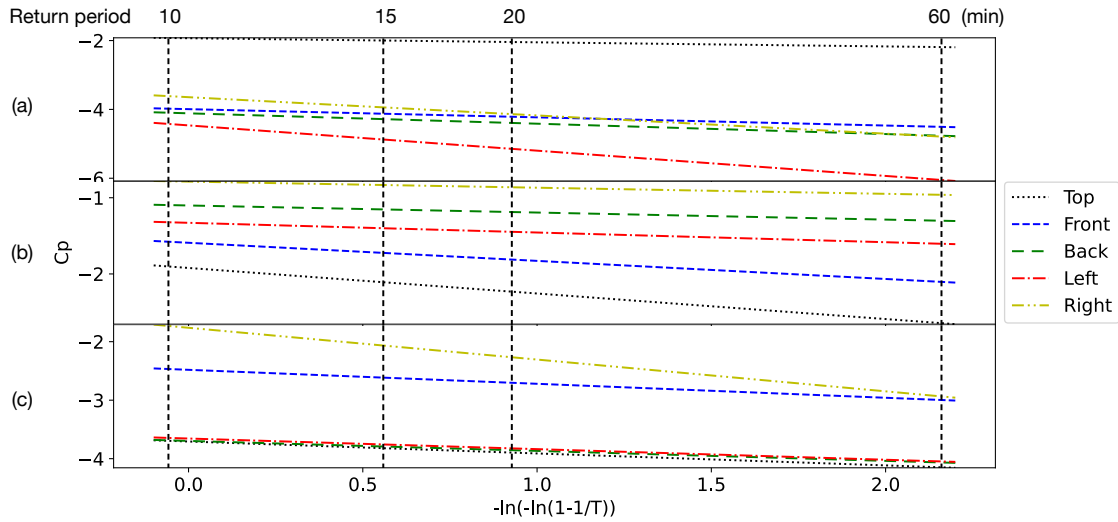


Figure 7. Return period for selected pressure taps (one on each face) for configuration 1, for (a) Shelter; (b) Cottage A and (c) Community Building. Vertical dotted lines indicate pressure coefficient return periods of 10, 15, 20 and 60 minutes, respectively.

pending on the effective wind area, but smaller tributary areas correspond to higher pressure deficits. These specification values are comparable to the range of observed C_p . Some further analyses will be performed in order to present a more detailed comparison between our results and ASCE 7-22 provisions to address its adequacy.

CONCLUSION

A novel wind chamber study of tornadic effects on different configurations of a complex, realistic community is conducted at the WindEEE Dome tornado simulator. 6 configurations of the KP community were subject to EF1-, EF2- and EF3-rated stationary TLVs. Pressure readings were collected and analyzed. We examined both time-averaged pressure coefficients $\overline{C_p}$ and instantaneous pressure coefficients. In all cases, the magnitude of C_p decreases as the swirl ratio increases. The explanation for this observation has not been unanimous from previous studies performed without buildings, and could be due to either the velocity used in assessing the dynamic pressure, or a physical change of the TLV structure. Further analyses need to be conducted to explain these discrepancies in terms of aerodynamic building effects. Varying building geometries produced some observable effects caused by building interaction, notably by the removal or addition of auxiliary structures on the Shelter building.

3-second averages of the instantaneous C_p were then binned, and fit to a Gumbel distribution to retrieve extreme C_p values and to assess pressure return period values. Analyses still need to be performed to assess the peak C_p and return period values to ASCE 7-22 provisions. Some preliminary works have been done in assessing the ASCE 7-22 design pressures, however challenges remain given the complex geometries of KP buildings, which do not fit the archetypes laid out by the code. In addition, we plan to analyze total forces exerted by the buildings, and also compare them with the building codes to highlight deficiencies and to improve tornado resilience.

REFERENCES

ASCE (2022). "Minimum design loads and associated criteria for buildings and other structures." *American Society of Civil Engineers*.

Blair, S. F. and Leighton, J. W. (2014). "Assessing real-time tornado information disseminated through NWS products." *Weather and Forecasting*, volume 29, pp. 591–600.

Ginger, J. and Letchford, C. (1993). "Characteristics of large pressures in regions of flow separation." *Journal of Wind Engineering and Industrial Aerodynamics*, volume 49, pp. 301–310.

Godlewski, T., Wodzyński, L., and Wszedyrówny-Nast, M. (2021). "Probabilistic analysis as a method for ground freezing depth estimation." *Applied Sciences*, volume 11.

Haan, F. L., Balaramudu, V. K., and Sarkar, P. P. (2010). "Tornado-induced wind loads on a low-rise building." *Journal of Structural Engineering*, volume 136, pp. 106–116.

Hadavi, M., Sun, L., and Romanic, D. (2022). "Normalized insured losses caused by windstorms in Quebec and Ontario, Canada, in the period 2008–2021." *International Journal of Disaster Risk Reduction*, volume 80, p. 103222.

Hangan, H., Refan, M., Jubayer, C., et al. (2017). "Novel techniques in wind engineering." *Journal of Wind Engineering and Industrial Aerodynamics*, volume 171, pp. 12–33.

Hong, H. P., Li, S. H., and Mara, T. G. (2013). "Performance of the generalized least-squares method for the Gumbel distribution and its application to annual maximum wind speeds." *Journal of Wind Engineering and Industrial Aerodynamics*, volume 119, pp. 121–132.

ISO 4354:2009 (2000). "Wind actions on structures." *Standard*, International Organization for Standardization, Geneva, CH.

Lewellen, D. C. and Lewellen, W. S. (2007). "Near-surface intensification of tornado vortices." *Journal of the Atmospheric Sciences*, volume 64, pp. 2176–2194.

Lieblein, J. (1976). "Efficient methods of extreme-value methodology." *NEA*.

Lin, J.-X., Surry, D., and Tieleman, H. (1995). "The distribution of pressure near roof corners of flat roof low buildings." *Journal of Wind Engineering and Industrial Aerodynamics*, volume 56, pp. 235–265.

Lombardo, F. T., Roueche, D. B., and Prevatt, D. O. (2015). "Comparison of two methods of near-surface wind speed estimation in the 22 May, 2011 Joplin, Missouri tornado." *Journal of Wind Engineering and Industrial Aerodynamics*, volume 138, pp. 87–97.

Narancio, G., Romanic, D., Chowdhury, J., et al. (2023a).

- “Can pressure coefficients obtained from ABL wind tunnel be used for tornadoes.” International Wind Engineering Conference (ICWE 16), Florence, Italy.
- Narancio, G., Romanic, D., Chowdury, J., *et al.* (2023b). “An appraisal of tornado-induced load provisions in ASCE/SEI 7-22 and 7-16 for residential low-rise buildings.” *Civil and Environmental Engineering Publications*, volume 204.
- Nolan, D. S. (2013). “On the use of doppler radar-derived wind fields to diagnose the secondary circulations of tornadoes.” *Journal of the Atmospheric Sciences*, volume 70, p. 1160–1171.
- Refan, M. and Hangan, H. (2018). “Near surface experimental exploration of tornado vortices.” *Journal of Wind Engineering and Industrial Aerodynamics*, volume 175, pp. 120–135.
- Romanic, D., Kassab, A., Chowdhury, J., *et al.* (2023a). “An analysis of the influence of a generic building on tornadic flow fields using high-frequency PIV and point velocity measurements.” *Journal of Fluids and Structures*, volume 123, p. 104010.
- Romanic, D., Parvu, D., Refan, M., and Hangan, H. (2018). “Wind and tornado climatologies and wind resource modelling for a modern development situated in “Tornado Alley”.” *Renewable Energy*, volume 115, pp. 97–112.
- Romanic, D., Refan, M., Wu, C., and Michel, G. (2016). “Oklahoma tornado risk and variability: A statistical model.” *International Journal of Disaster Risk Reduction*, volume 16, pp. 19–32.
- Romanic, D., Shoji, H., and Hangan, H. (2023b). “Experimental investigation of surface pressures, velocities, and dynamic structural analysis of tornadic winds on a luminary pole.” *Journal of Fluids and Structures*, volume 116, p. 103794.
- Roueche, D. B., Prevatt, D. O., and Haan, F. L. (2020). “Tornado-induced and straight-line wind loads on a low-rise building with consideration of internal pressure.” *Frontiers in Built Environment*, volume 6.
- Sabareesh, G. R., Cao, S., Wang, J., *et al.* (2018). “Effect of building proximity on external and internal pressures under tornado-like flow.” *Wind and Structures*, volume 26, p. 163–177.
- Stathopoulos, T., Baskaran, A., and Goh, P. (1990). “Full-scale measurements of wind pressures on flat roof corners.” *Journal of Wind Engineering and Industrial Aerodynamics*, volume 36, pp. 1063–1072.
- Wang, J. and Cao, S. (2021). “Characteristics of tornado wind loads and examinations of tornado wind load provisions in ASCE 7–16.” *Engineering Structures*, volume 241, p. 112451.